1521-009X/44/12/1963–1972$25.00
Drug Metabolism and Disposition

https://doi.org/10.1124/dmd.116.071902
Drug Metab Dispos 44:1963–1972, December 2016

Tramadol Metabolism to *O*-Desmethyl Tramadol (M1) and *N*-Desmethyl Tramadol (M2) by Dog Liver Microsomes: Species Comparison and Identification of Responsible Canine Cytochrome P450s

Tania E. Perez, Katrina L. Mealey, Tamara L. Grubb, Stephen A. Greene, and Michael H. Court

Program in Individualized Medicine, Pharmacogenomics Laboratory, Department of Veterinary Clinical Sciences, Washington State University College of Veterinary Medicine, Pullman, Washington

Received June 3, 2016; accepted October 5, 2016

ABSTRACT

Tramadol is widely used to manage mild to moderately painful conditions in dogs. However, this use is controversial, since clinical efficacy studies in dogs showed conflicting results, whereas pharmacokinetic studies demonstrated relatively low circulating concentrations of *O*-desmethyltramadol (M1). Analgesia has been attributed to the opioid effects of M1, whereas tramadol and the other major metabolite (*N*-desmethyltramadol, M2) are considered inactive at opioid receptors. This study aimed to determine whether cytochrome P450 (P450)–dependent M1 formation by dog liver microsomes is slower compared with cat and human liver microsomes and to identify the P450s responsible for M1 and M2 formation in canine liver. Since tramadol is used as a racemic mixture of (+)- and (−)-stereoisomers, both (+)-tramadol and (−)-tramadol were evaluated as substrates. M1 formation from tramadol by liver microsomes from dogs was slower than from cats (3.9-fold) but faster than humans (7-fold). However, M2 formation by liver microsomes from dogs was faster than those from cats (4.8-fold) and humans (19-fold). Recombinant canine P450 activities indicated that M1 was formed by CYP2D15, whereas M2 was largely formed by CYP2B11 and CYP3A12. This was confirmed by dog liver microsome studies that showed selective inhibition of M1 formation by quinidine and M2 formation by chloramphenicol and CYP2B11 antiserum, as well as induction of M2 formation by phenobarbital. Findings were similar for both (+)-tramadol and (−)-tramadol. In conclusion, low circulating M1 concentrations in dogs are explained in part by low M1 formation and high M2 formation, which is mediated by CYP2D15 and CYP2B11/CYP3A12, respectively.

Introduction

Tramadol is an orally active drug that is widely used in the management of mild to moderately painful conditions in dogs (Gaynor, 2008; Lamont, 2008). However, this use in dogs is controversial, since clinical efficacy studies have produced conflicting results. Some studies indicate that tramadol is equally or more effective than other drugs used to treat pain in dogs (Mastrocinque and Fantoni, 2003; Almeida et al., 2010; Martins et al., 2010; Clark et al., 2011; KuKanich and Papich, 2011; Malek et al., 2012; Neves et al., 2012; Rialland et al., 2012; Kongara et al., 2013; Morgaz et al., 2013; Teixeira et al., 2013; Cardozo et al., 2014), whereas other studies have shown relatively poor analgesic efficacy in dogs (Davila et al., 2013; Delgado et al., 2014; Kögel et al., 2014). Tramadol is considered a prodrug with regard to opioid analgesic effects, requiring metabolic activation by cytochrome P450 (P450) enzymes. Consequently, variability in drug response between studies could be a consequence of genetic polymorphisms or drug–drug interactions involving the canine P450s. However, the P450s responsible for metabolizing tramadol to its active metabolite in dogs are unknown.

In humans, tramadol is primarily metabolized in the liver to *O*-desmethyltramadol (M1) by CYP2D6 and to *N*-desmethyltramadol (M2) by CYP2B6 and CYP3A4 (Fig. 1) (Subrahmanyam et al., 2001). The analgesic effects of tramadol are primarily attributed to μ-opioid receptor activation by the M1 metabolite (KuKanich and Papich, 2004), whereas both tramadol and M2 are essentially devoid of opioid agonist effects (Lai et al., 1996; Gillen et al., 2000). The importance of CYP2D6-dependent metabolic activation of tramadol to M1 for analgesia has been demonstrated (in part) by studies of humans with CYP2D6 polymorphisms. In one study, patients with the CYP2D6 poor-metabolizer phenotype required higher tramadol doses and needed rescue pain medication more often than patients with the CYP2D6 extensive-metabolizer phenotype (Stamer et al., 2003). Several other studies in human volunteers have also shown that the (opioid-dependent) miotic effects of tramadol and M1 plasma concentrations increase in proportion to CYP2D6 enzyme activity (Fliegert et al., 2005; Slanar et al., 2007; Matouskova et al., 2011).

Tramadol and the M1 and M2 metabolites have two chiral centers in the cyclohexane ring (see Fig. 1). All currently available pharmaceutical formulations of tramadol are a racemic mixture of (+)-(1*R*,2*R*)-tramadol

This research was supported by the Morris Animal Foundation [Fellowship Training Grant D16CA-401 (to T.E.P.)], the National Institutes of Health National Institute of General Medical Sciences [Grant R-01-GM102130 (to M.H.C.)], and the William R. Jones Endowment to Washington State University College of Veterinary Medicine.

https://doi.org/10.1124/dmd.116.071902.

ABBREVIATIONS: ANOVA, analysis of variance; DLM, dog liver microsome; HPLC, high-performance liquid chromatography; *m/z*, mass-to-charge ratio; M1, *O*-desmethyltramadol; M2, *N*-desmethyltramadol; MS, mass spectrometry; P450, cytochrome P450.

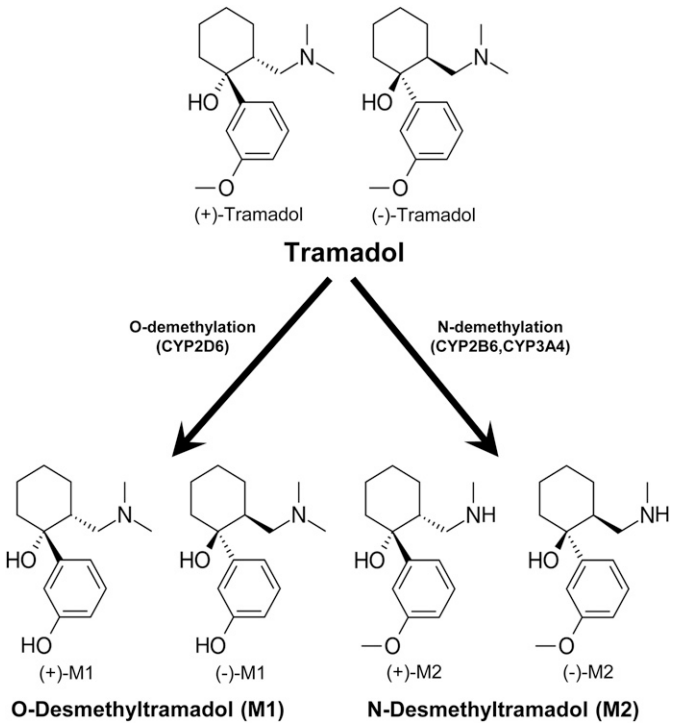

Fig. 1. Tramadol metabolic pathways evaluated in this study. Tramadol and the M1 and M2 metabolites have two chiral centers in the cyclohexane ring. All pharmaceutical preparations of tramadol are a racemic mixture of (+)-(1*R*,2*R*)-tramadol and (−)-(1*S*,2*S*)-tramadol, also known as (+)-tramadol and (−)-tramadol, respectively. In humans, racemic tramadol is *O*-demethylated by CYP2D6 to *O*-desmethyltramadol (M1) and *N*-demethylated by CYP2B6 and CYP3A4 to *N*-desmethyltramadol (M2).

and (−)-(1*S*,2*S*)-tramadol, also known as (+)-tramadol and (−)-tramadol, respectively. Interestingly, (+)-M1 appears to be a more effective μ-opioid agonist than (−)-M1 (Raffa et al., 1993). This was supported by a clinical study that showed about 2-fold lower (+)-tramadol and (+)-M1 plasma concentrations required for analgesia in human patients administered pure (+)-tramadol compared with plasma concentrations of (−)-tramadol and (−)-M1 in patients who were administered pure (−)-tramadol (Grond et al., 1999). However, studies of tramadol metabolism by recombinant P450s thus far have used only racemic (±)-tramadol, so it is unclear whether (+)-tramadol and (−)-tramadol are metabolized to their respective M1 and M2 metabolite stereoisomers by different P450s or at different rates by specific P450s (Subrahmanyam et al., 2001).

Dogs may differ in the capacity to metabolize tramadol to M1 compared with other species. Specifically, pharmacokinetic studies have shown that average M1/tramadol area under the plasma concentration versus time curve ratios after tramadol administration to dogs (0.027–0.1; Giorgi et al., 2009; KuKanich and Papich, 2011) are quite low compared with humans (0.27; García Quetglas et al., 2007; García-Quetglas et al., 2007) and cats (1.4; Cagnardi et al., 2011), suggesting that dogs may form M1 less efficiently than humans or cats. Tramadol is also commonly used to treat pain in cats. In contrast with dogs, studies in cats (although fewer) have consistently demonstrated efficacy (Pypendop et al., 2009; Evangelista et al., 2014), which may be a consequence of the relatively high circulating M1 concentrations reported in cats after tramadol administration (Pypendop et al., 2009; Cagnardi et al., 2011).

In this study, we initially evaluated species differences in hepatic microsomal metabolism of racemic (±)-tramadol to M1 and M2 to test the hypothesis that M1 formation (relative to M2 formation) is slower in dog liver microsomes (DLMs) compared with cat and human liver microsomes. We then used multiple approaches (recombinant enzymes, chemical and antibody inhibition, and induced hepatic microsomes) to identify the P450s responsible for metabolizing (+)-tramadol and (−)-tramadol to M1 and M2 in dog liver. We hypothesized that M1 would be formed by CYP2D15 (the canine ortholog of human CYP2D6) and that M2 would be formed by CYP2B11 and CYP3A12 (the canine orthologs of human CYP2B6 and CYP3A4).

Materials and Methods

Reagents. The following were purchased from Toronto Research Chemicals Inc. (Toronto, ON, Canada): (+)-tramadol hydrochloride, (−)-tramadol hydrochloride, *O*-desmethyltramadol hydrochloride, *O*-desmethyltramadol-D6, *N*-desmethyltramadol, and *N*-desmethyltramadol-D3 hydrochloride. Racemic (±)-tramadol was made by combining equal amounts of (+)-tramadol and (−)-tramadol. $NADP^+$, isocitrate dehydrogenase, DL-isocitrate, chloramphenicol, and quinidine were obtained from Sigma-Aldrich (St. Louis, MO).

Bactosomes expressing recombinant canine P450s (CYP1A1, CYP1A2, CYP2B11, CYP2C21, CYP2C41, CYP2D15, CYP3A12, and CYP3A26; each coexpressed with canine P450 oxidoreductase) and liver microsomes from male Beagle dogs treated with corn oil, rifampin, β-naphthoflavone, saline, phenobarbital, and clofibric acid were obtained from Xenotech LLC (Lenexa, KS). Liver microsomes were prepared as previously described (Court et al., 1997) from a bank of frozen dog livers maintained at Washington State University (Pullman, WA). Livers were from 27 untreated adult dogs, including 5 Beagles (all males), 5 Greyhounds (all males), 12 mixed breed dogs (6 females and 6 males), 4 Chihuahuas (3 males and 1 female), and 1 Labrador Retriever (male). All dogs were healthy and were being euthanized for reasons unrelated to this study. Liver microsomes were prepared from a bank of frozen cat livers maintained at Washington State University that were obtained from 16 domestic short-haired cats (11 males and 5 females). The collection of the dog and cat livers was approved by the Institutional Animal Care and Use Committee Washington State University (no. 04412).

Microsomes were prepared using frozen liver samples from 48 human donors with no known liver disease, which were provided by the International Institute for the Advancement of Medicine (Exton, PA), the Liver Tissue Procurement and Distribution System (University of Minnesota, Minneapolis, MN), or the National Disease Research Interchange (Philadelphia, PA). These were deidentified samples that had originally been obtained under the approval of the Human Investigation Review Committee at the respective institutions. The use of these deidentified tissues for this study was approved by the Human Investigation Review Board at Washington State University.

The bicinchoninic acid assay (Thermo Scientific Pierce, Rockford, IL) was used to measure the microsomal protein content of the human, dog, and cat liver microsomes used in this study.

Tramadol Metabolism Assay Using Liver Microsomes and Recombinant P450s. An assay was developed to measure the rate of formation of M1 and M2 from tramadol [(+)-tramadol, (−)-tramadol, or (±)-tramadol] by dog, cat, and human liver microsomes and recombinant dog P450s. Briefly, 100-μl incubations contained an NADPH-regenerating system in phosphate buffer in water and enzyme (20 μg liver microsomes or 1 pmol recombinant enzyme) and was started by adding tramadol (1–2000 μM final concentration) in 50 mM potassium phosphate buffer (pH 7.4) in water. All samples were prepared in duplicate or triplicate and incubated for 10 minutes in a water bath at 37°C. The reaction was stopped by adding 100 μl ice-cold internal standards (200 nmol *O*-desmethyltramadol-D6 and 100 nmol *N*-desmethyltramadol-D3) in methanol, vortexed, and centrifuged at 13,000 relative centrifugal force for 5 minutes. The supernatant was analyzed by high-performance liquid chromatography (HPLC) with mass spectrometry (MS) detection. Unless otherwise indicated, all experiments were performed at least twice on different days and results were averaged.

The HPLC apparatus (Agilent 1100; Agilent Technologies, Santa Clara, CA) was connected to a triple quadrupole MS detector (AB Sciex API4000; Applied Biosystems Life Technologies, Framingham, MA) operated in positive ion mode. The mobile phase consisted of 65% (v/v) water [containing 0.1% (v/v) formic acid] and 35% (v/v) methanol that was pumped at 1 ml/min through a Zorbax

Eclipse XDB-C18 column (2.1 mm × 50 mm, 5 μm; Phenomenex, Torrance, CA). Mass transitions monitored included the following: mass-to-charge ratio (*m/z*) 264 → 58 (tramadol), *m/z* 250 → 58 (*O*-desmethyltramadol), *m/z* 250 → 44 (*N*-desmethyltramadol), *m/z* 256 → 64 (*O*-desmethyltramadol-D6), and *m/z* 253 → 47 (*N*-desmethyltramadol-D3). Retention times for *O*-desmethyltramadol, *O*-desmethyltramadol-D6, *N*-desmethyltramadol, *N*-desmethyltramadol-D3, and tramadol were 1.841, 1.833, 3.35, 3.331, and 2.87 minutes, respectively. The amount of metabolite formed per minute per milligram of liver microsome (or per picomole of P450) were calculated using a standard curve generated using samples with known concentrations of *O*-desmethyltramadol, *N*-desmethyltramadol, and internal standards dissolved in a blank matrix. Preliminary experiments confirmed linearity in metabolite formation for microsomal protein concentrations up to 0.2 mg/ml and incubation time up to 10 minutes.

Although this assay does not distinguish between the (+)- or (−)-metabolite enantiomers, the formation of each metabolite enantiomer from the respective substrate [(+)- or (−)-tramadol] was assumed based on evidence from at least one study that showed that the pure (+)- and (−)-enantiomers of tramadol and *O*-desmethyltramadol do not racemize (Grond et al., 1999).

Inhibition Assays. Chloramphenicol and quinidine were evaluated as inhibitors of M1 and M2 formation in pooled DLMs and recombinant enzymes. Inhibitors dissolved in methanol at concentrations ranging from 0.01 to 1000 μM were added to incubation tubes and dried down in a centrifugal vacuum. NADPH cofactor mix and enzyme (20 μg DLMs or 1 pmol recombinant CYP2B11or CYP2D15) were added to the tube and preincubated at 37°C for 15 minutes. Tramadol (5 μM final concentration) was then added and incubated for a further 10 minutes. The reaction was stopped by adding internal standard and the metabolites formed were measured by HPLC as described above.

An antibody inhibition assay was performed using rabbit anti-CYP2B11 immune serum that was a gift from Dr. James Halpert (School of Pharmacy, University of Connecticut, Storrs, CT) (Duignan et al., 1987). Pooled DLMs (0.2 mg/ml final concentration) were preincubated with the serum at different

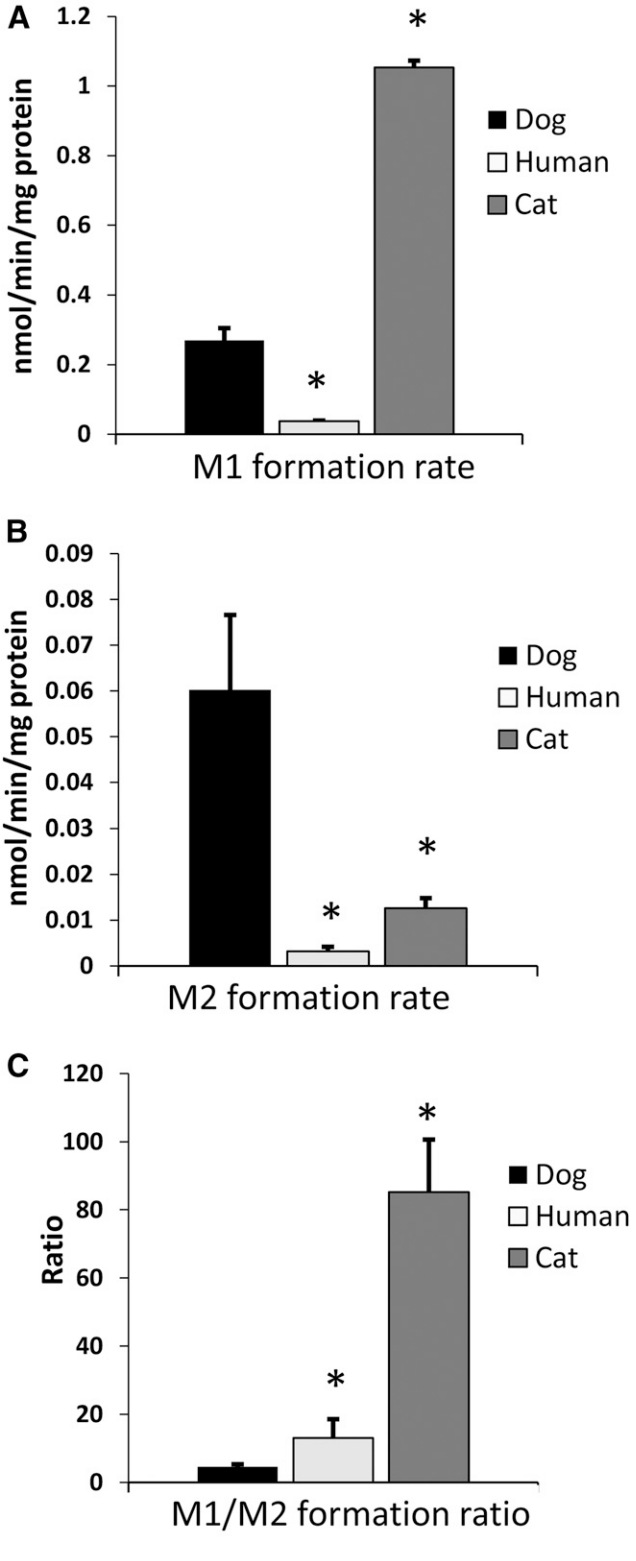

Fig. 2. Species differences in formation rates of M1 (A) and M2 (B) and in the ratios of M1/M2 (C) from racemic (±)-tramadol by pooled dog (n = 27), human (n = 48), and cat (n = 16) liver microsomes. Bars represent the mean ± S.D. of triplicate independent determinations. *$P < 0.001$ versus DLMs (ANOVA with the Tukey test).

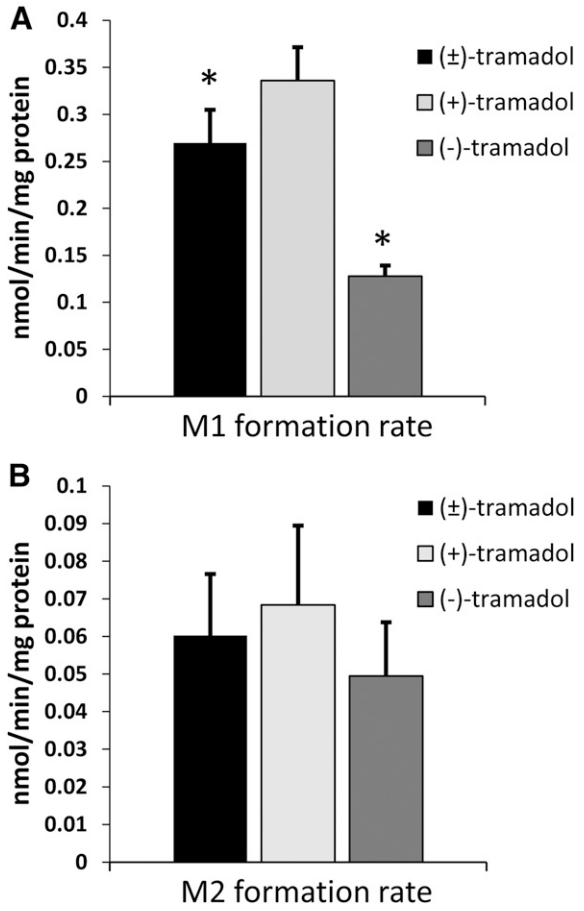

Fig. 3. Formation rates of M1 (A) and M2 (B) from racemic (±)-tramadol, (+)-tramadol, and (−)-tramadol by pooled (n = 27) DLMs. Bars represent the mean ± S.D. of triplicate independent determinations. *$P < 0.001$ versus DLMs (ANOVA with the Tukey test).

concentrations (ratios of serum to microsomal protein were 0:1, 5:1, 10:1, 15:1, and 20:1) for 30 minutes at room temperature with NADPH cofactor mix. Tramadol (5 μM final concentration) was then added and incubated for a further 10 minutes. The reaction was stopped by adding internal standard and metabolites measured by HPLC-MS as described above.

For all inhibition assays, samples were prepared in triplicate, and M1 and M2 formation rates were averaged and then expressed as a percentage of control incubations that lacked inhibitor.

Enzyme Kinetic and Statistical Analyses. Kinetic and statistical analyses were performed using SigmaPlot 12 software (Systat Software Inc., San Jose, CA). For enzyme kinetic analysis, enzyme kinetics parameters (K_m and V_{max}) were determined using either the one-enzyme or two-enzyme Michaelis–Menten model using nonlinear regression analysis. The model of best fit was evaluated based on plots of fitted versus observed data. Half-maximal inhibitory concentration (IC_{50}) values were determined using nonlinear regression with a four-parameter logistic curve. Differences in enzyme activities were evaluated using an unpaired *t* test (two groups) or analysis of variance (ANOVA; three groups) with post hoc pairwise comparisons using the Tukey test after first verifying prerequisites for parametric testing, including the normality of data distribution and equal variance between groups.

Results

Racemic (±)-Tramadol Metabolism by Dog, Human, and Cat Liver Microsomes. Racemic (±)-tramadol was incubated at a 5-μM substrate concentration with pooled liver microsomes from dogs (n = 27), humans (n = 48), and cats (n = 16) to evaluate species differences in tramadol metabolism. This substrate concentration was chosen since it roughly approximated maximal plasma concentrations (range, 0.3–8 μM) observed in pharmacokinetic studies of tramadol in dogs administered at clinically used dosages (KuKanich and Papich, 2004, 2011; Giorgi et al., 2009). Mean (± S.D.) M1 and M2 formation rates and M1 to M2 formation ratios for each substrate are shown in Fig. 2. DLMs showed 3.9-fold lower M1 formation rates than cat liver microsomes ($P < 0.001$, ANOVA with the Tukey test) but over 7-fold higher activities than human liver microsomes ($P < 0.001$) (Fig. 2A). On the other hand (Fig. 2B), DLMs showed consistently higher M2 formation rates than both cat liver microsomes (by 4.8-fold; $P < 0.001$) and human liver microsomes (by 19-fold; $P < 0.001$). When expressed as a M1/M2 metabolite ratio (Fig. 2C), DLMs formed the lowest amount of M1 relative to M2, about 2.8-fold less than human liver microsomes ($P < 0.001$) and 19-fold less than cat liver microsomes.

Tramadol Enantiomer Metabolism by DLMs. (±)-Tramadol, (+)-tramadol, and (−)-tramadol were then incubated at the 5-μM substrate concentration with pooled DLMs to evaluate stereoselectivity in M1 and M2 formation. As shown in Fig. 3A, formation of M1 from (+)-tramadol was about 2.6-fold higher than from (−)-tramadol ($P < 0.001$, ANOVA with the Tukey test), whereas M1 formation from (±)-tramadol was intermediate between (+)-tramadol and (−)-tramadol. However, there were no differences in M2 formation from (±)-tramadol, (+)-tramadol, or (−)-tramadol (Fig. 3B).

Enzyme kinetic analysis was used to evaluate differences in the capacity of DLMs to form the M1 and M2 metabolites over a wide range of (+)-tramadol and (−)-tramadol concentrations (up to 2000 μM). Plots of M1 and M2 formation from (+)-tramadol and (−)-tramadol by pooled

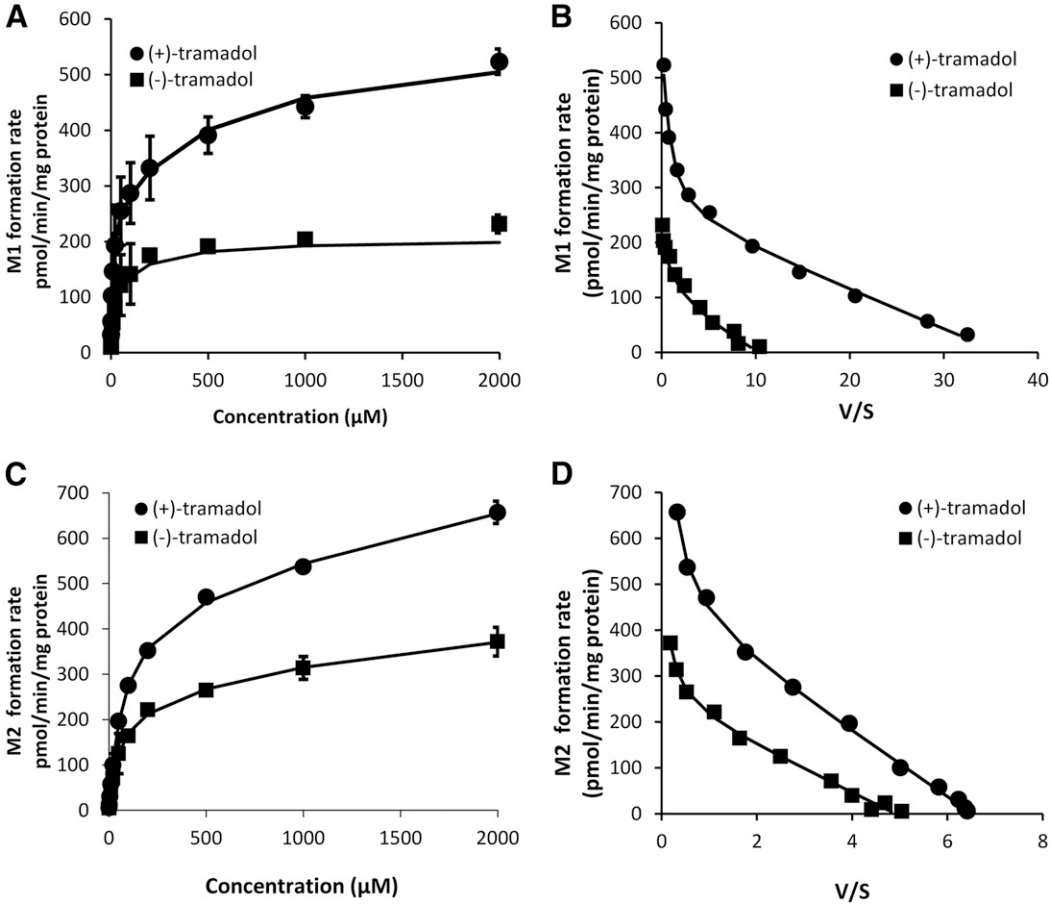

Fig. 4. Michaelis–Menten enzyme kinetic plots of M1 (A) and M2 (C) formation from (+)-tramadol and from (−)-tramadol by pooled (n = 27) DLMs. Also shown are Eadie-Hofstee plots of these same data (B and D, respectively). Each data point represents the mean of two independent determinations performed in duplicate, and the curves represent the model of best fit to the data. V/S, reaction velocity divided by substrate concentration.

TABLE 1

Enzyme kinetic parameters determined by nonlinear regression for formation of M1 and M2 from (+)-tramadol and (−)-tramadol by pooled DLMs (n = 27)

Activity	High-Affinity Activity			Low-Affinity Activity			
	K_m	V_{max}	V_{max}/K_m	K_m	V_{max}	V_{max}/K_m	$\Sigma V_{max}/K_m$
	μM	*pmol/min per mg protein*	*ml/min per g protein*	*μM*	*pmol/min per mg protein*	*ml/min per g protein*	
(+)-M1	7.0	248	35	554	329	0.6	36
(−)-M1	9.8	92	9.3	117	13	0.11	9.4
(+)-M2	69	440	6.4	5442	843	0.15	6.6
(−)-M2	49	235	4.6	2494	318	0.12	4.7

The data points used for fitting were the average of two independent experiments performed in duplicate (data points shown in Fig. 4 with the curves of best fit). Fitted parameters included K_m and V_{max}, while intrinsic clearance (V_{max}/K_m) values were calculated. Data for (+)-M1 and (−)-M1 formation were best fit by a two-enzyme model. Kinetic parameters for high- and low-affinity activities, as well as the sum of the high and low intrinsic clearance values ($\Sigma V_{max}/K_m$), are given.

DLMs are shown in Fig. 4 and derived kinetic parameters are presented in Table 1. Eadie-Hofstee plots were clearly biphasic for M1 and M2 formation from (+)-tramadol and (−)-tramadol, consistent with the contribution of distinct high- and low-affinity activities in DLMs. The M1 formation intrinsic clearance estimate for the high-affinity activity was 2.7 times higher for (+)-tramadol compared with (−)-tramadol, whereas M1 formation intrinsic clearance for the low-affinity activity was about 5.5 times higher for (+)-tramadol compared with (−)-tramadol (Table 1). Intrinsic clearance values were similar for formation of M2 from (+)-tramadol compared with (−)-tramadol for both high- and low-affinity activities.

Tramadol Enantiomer Metabolism by Recombinant Dog P450s. (+)-Tramadol and (−)-tramadol at the 5- and 100-μM concentrations were incubated with all commercially available recombinant dog P450s to identify which canine P450s are capable of forming M1 and M2 from (+)-tramadol and (−)-tramadol. As shown in Fig. 5, A and C, only CYP2D15 showed significant formation of M1 from (+)-tramadol and (−)-tramadol, >30 times higher than the next most active P450

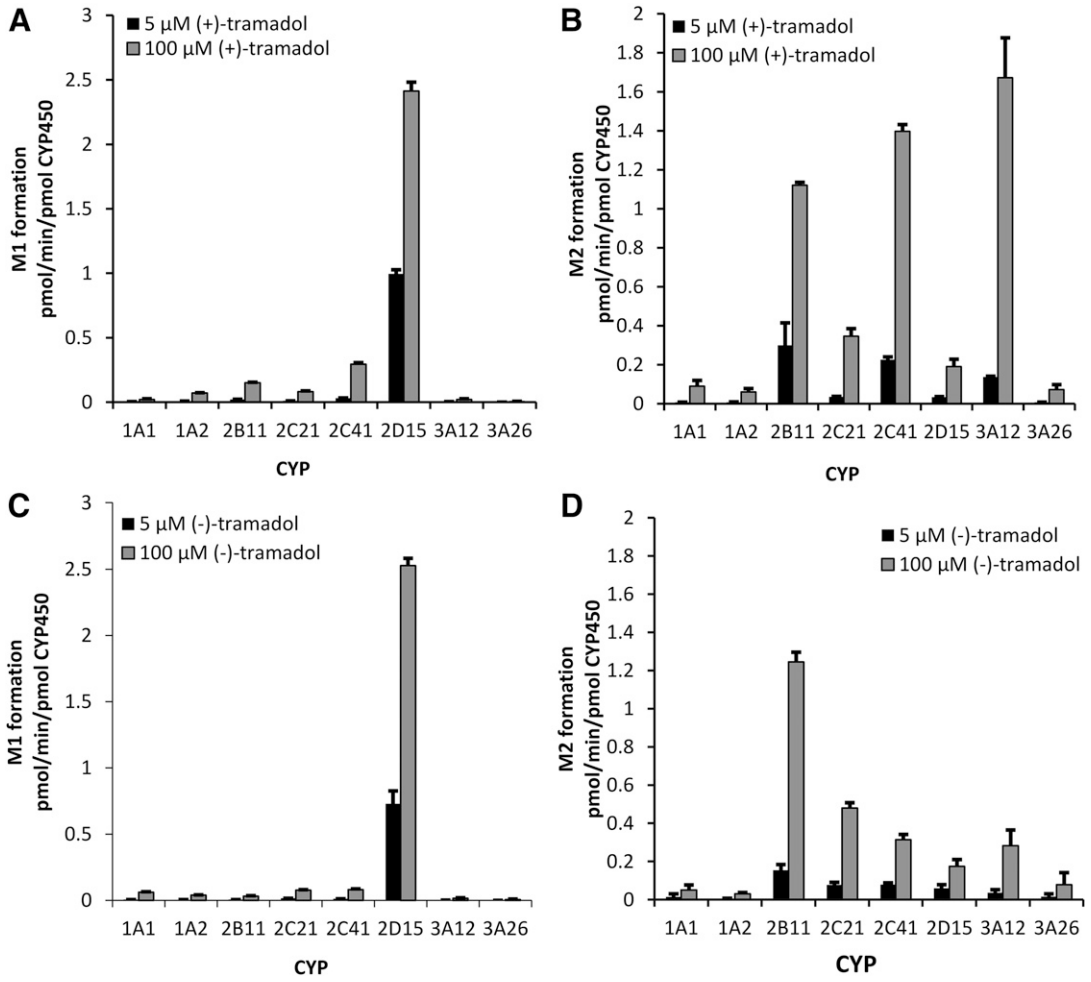

Fig. 5. Formation rates of M1 (A and C) and M2 (B and D) from (+)-tramadol (A and B) and from (−)-tramadol (C and D) by recombinant canine P450s measured at the 5- and 100-μM substrate concentrations. Bars represent the mean ± S.D. of triplicate determinations. CYP, cytochrome P450.

(CYP2B11) at both 5- and 100-μM concentrations. On the other hand, M2 formation from both (+)-tramadol and (−)-tramadol was mediated by multiple P450s, including CYP2B11, CYP2C41, CYP2C21, CYP3A12, and CYP2D15 (Fig. 5, B and D). However, at the lower concentration tested (5 μM), CYP2B11 was the most active enzyme for both (+)-tramadol and (−)-tramadol.

Enzyme kinetic analysis was then performed using the recombinant P450s that showed the highest formation rates of M1 (CYP2D15) and M2 (CYP2B11, CYP2D15, CYP2C41, CYP2C21, and CYP3A12) to evaluate differences in the overall capacity to metabolize (+)-tramadol and (−)-tramadol. Plots of M1 formation from both (+)-tramadol and (−)-tramadol by CYP2D15 are shown in Fig. 6, A and B, whereas plots of M2 formation from both (+)-tramadol and (−)-tramadol by CYP2B11 are shown in Fig. 6, C and D. Derived enzyme kinetic parameters from all P450s evaluated are given in Table 2. Eadie-Hofstee plots showed monophasic kinetics for most activities evaluated. Exceptions that were best described by biphasic kinetics included M1 formation from (+)-tramadol and (−)-tramadol by CYP2D15, as well as M2 formation from (+)-tramadol and (−)-tramadol by CYP2B11. Total intrinsic clearance estimates for M1 formation from (+)-tramadol and (−)-tramadol were 125-fold and 155-fold higher, respectively, for CYP2D15 compared with CYP2B11. On the other hand, total intrinsic clearance estimates for M2 formation from (+)-tramadol and (−)-tramadol were substantially lower for CYP2D15 compared with all other P450s evaluated. M2 formation from (+)-tramadol was highest for CYP2C41, CYP3A12, and CYP2B11, whereas M2 formation from (−)-tramadol was highest for CYP2B11.

To explain higher M1 formation by DLMs from (+)-tramadol compared with (−)-tramadol, we then compared high- and low-affinity intrinsic clearance estimates for M1 formation by CYP2D15 for each enantiomer. Interestingly a similar pattern to that observed for DLMs was seen with CYP2D15, in that the M1 formation intrinsic clearance estimate for the high-affinity activity was 4.6 times higher for (+)-tramadol compared with (−)-tramadol, whereas the low-affinity activity intrinsic clearance estimate was 1.5 times higher for (+)-tramadol compared with (−)-tramadol (Table 2).

Relative Contribution of P450s to M1 and M2 Formation. The relative contributions of each canine P450 to total formation of M1 and M2 in the liver were then calculated using the measured intrinsic clearance estimates from Table 2 and were normalized to hepatic P450 content using average published estimates (Heikkinen et al., 2015) that were available for CYP2B11 (35 pmol/mg protein), CYP2C21 (70 pmol/mg protein), CYP2D15 (56 pmol/mg protein), and CYP3A12 (93 pmol/mg protein) in Beagle liver microsomes. Unfortunately, an estimate of CYP2C41 hepatic abundance was not available. As shown in Fig. 7, M1 was predominantly formed by CYP2D15 from both (+)-tramadol (99%) and (−)-tramadol (99%), with essentially no contribution from any other P450 evaluated (<1%). Conversely, M2

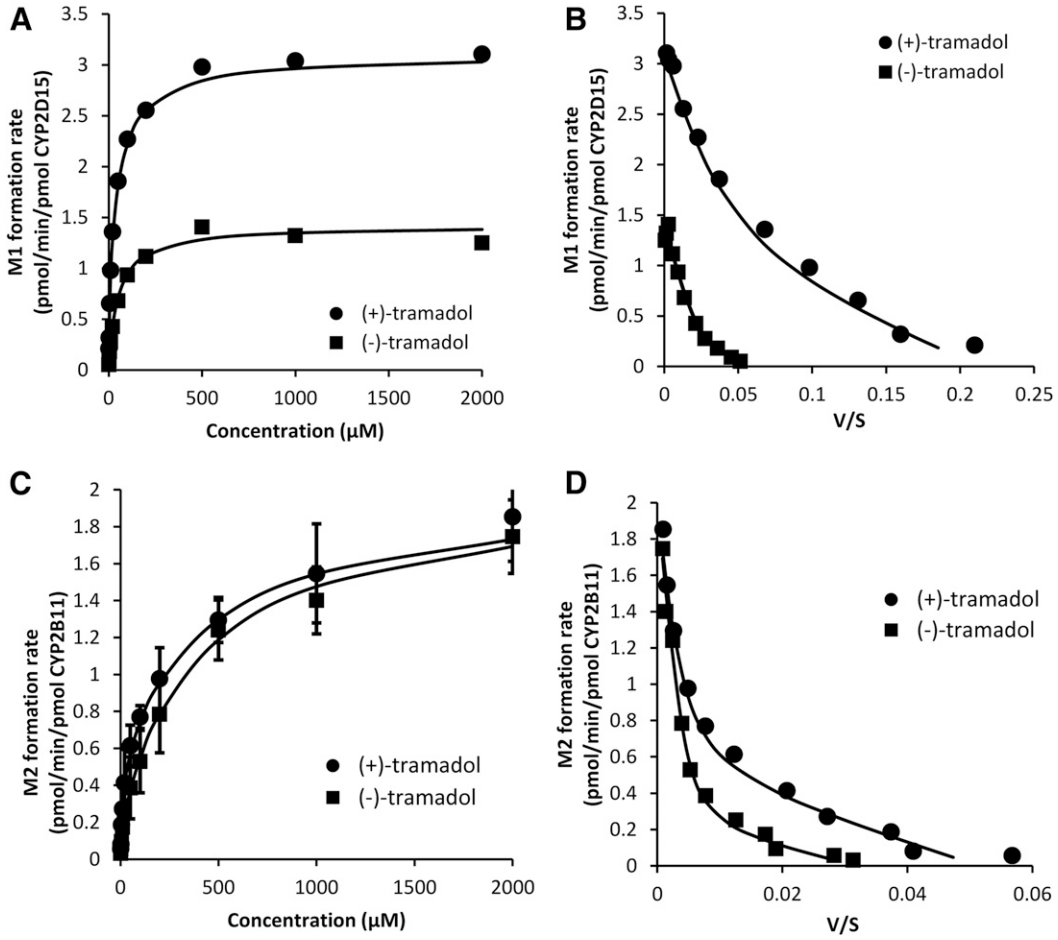

Fig. 6. Michaelis–Menten enzyme kinetic plots of M1 formation by CYP2D15 (A) and M2 formation by CYP2B11 (C) from (+)-tramadol and from (−)-tramadol. Also shown are Eadie-Hofstee plots of these same data (B and D, respectively). Each data point represents the mean of three independent determinations performed in duplicate, and the curves represent the model of best fit to the data. V/S, XXX

TABLE 2

Enzyme kinetic parameters determined by nonlinear regression for formation of M1 and M2 from (+)-tramadol and (−)-tramadol by dog recombinant P450s

Activity	P450	High-Affinity Activity			Low-Affinity Activity			
		K_m	V_{max}	V_{max}/K_m	K_m	V_{max}	V_{max}/K_m	$\Sigma V_{max}/K_m$
		μM	*pmol/min per pmol P450*	*μl/min per nmol P450*	*μM*	*pmol/min per pmol P450*	*μl/min per nmol P450*	
(+)-M1	CYP2D15	5.5	1.0	182	66	2.1	32	214
	CYP2B11	173	0.3	1.7				
(−)-M1	CYP2D15	3.0	0.12	40	59	1.3	22	62
	CYP2B11	445	0.18	0.4				
(+)-M2	CYP2B11	10.4	0.5	48	430	1.5	3.5	51.5
	CYP2D15	474	0.6	1.3				
	CYP2C21	30	0.4	13				
	CYP2C41	8.5	1.1	130				
	CYP3A12	23	1.5	65				
(−)-M2	CYP2B11	7.2	0.2	28	765	1.9	2.5	30.5
	CYP2D15	351	0.6	1.7				
	CYP2C21	68.5	0.3	4.4				
	CYP2C41	61	0.8	13				
	CYP3A12	55	0.4	7.3				

The data points used for fitting were the average of three independent experiments performed in duplicate (data points shown in Fig. 5 with the curves of best fit). Fitted parameters included K_m and V_{max}, while intrinsic clearance (V_{max}/K_m) values were calculated. Data for (+)-M1 and (−)-M1 formation by CYP2D15 were best fit by a two-enzyme model. Kinetic parameters for high- and low-affinity activities, as well as the sum of the high and low intrinsic clearance values ($\Sigma V_{max}/K_m$), are given.

was formed from (+)-tramadol and (−)-tramadol primarily by CYP2B11 (20% and 50%) and CYP3A12 (68% and 32%), with smaller contributions from CYP2C21 (10% and 14%) and negligible contributions from CYP2D15 (1% and 4%).

Effect of P450-Selective Chemical and Antiserum Inhibitors. The effects of selective inhibitors of CYP2D15 (quinidine; Roussel et al., 1998) and CYP2B11 (chloramphenicol; Hay Kraus et al., 2000) on M1 and M2 formation from (+)-tramadol and from (−)-tramadol in pooled DLMs and recombinant CYP2D15 and CYP2B11 were evaluated over a wide range of inhibitor concentrations from 0.01 to 1000 μM. As shown in Fig. 8, quinidine selectively inhibited M1 formation from (+)-tramadol for DLMs (IC_{50} = 0.25 ± 0.1 μM) and CYP2D15 (IC_{50} = 1.7 ± 0.17 μM), whereas chloramphenicol did not (IC_{50} > 50 μM for both). Conversely, chloramphenicol selectively inhibited M2 formation from (+)-tramadol for DLMs (IC_{50} = 1.2 ± 0.3 μM) and CYP2B11 (8.8 ± 0.25 μM), but quinidine did not (IC_{50} > 100 μM for both). Essentially identical results were observed for M1 formation from (−)-tramadol with inhibition by quinidine for DLMs (IC_{50} = 0.31 ± 0.18 μM) and CYP2D15 (IC_{50} = 1.6 ± 0.16 μM), but not by chloramphenicol (IC_{50} > 50 μM for both). Similarly, there was selective inhibition of M2 formation from (−)-tramadol by chloramphenicol for DLMs (IC_{50} = 0.88 ± 0.5 μM) and CYP2B11 (IC_{50} = 10.5 ± 0.03 μM), but not by quinidine (IC_{50} > 100 μM for both).

The effect of preincubation with increasing amounts of an inhibitory antiserum specific to CYP2B11 on M1 and M2 formation from (+)-tramadol and (−)-tramadol was evaluated using pooled DLMs. As shown in Fig. 9, there was selective inhibition (>50% decrease in mean activity from control) of M2 formation from (+)-tramadol and (−)-tramadol, without substantially affecting M1 formation from (+)-tramadol and (−)-tramadol at all CYP2B11 antiserum concentrations evaluated (antiserum/microsomal protein ratios of 5:1 to 20:1).

Effect of P450-Selective Inducers. The effect of P450-selective inducers including β-naphthoflavone (CYP1A), phenobarbital (CYP2B), rifampin (CYP3A), and clofibric acid (CYP4A) on tramadol metabolism was evaluated using pooled liver microsomes from male Beagle dogs (two per treatment) that had been administered each of these inducers. Results were compared with vehicle-treated liver microsomes. Vehicles included corn oil for rifampin and β-naphthoflavone and saline for phenobarbital and clofibric acid. As shown in Fig. 10, none of the inducers substantially affected M1 formation from (+)-tramadol or (−)-tramadol with <2-fold average differences from control activities. On the other hand, M2 formation from (+)-tramadol and from (−)-tramadol was substantially increased by phenobarbital, with mean activities that were 14.0 ± 0.02 and 14.4 ± 0.11 times control activities, respectively. None of the other inducers evaluated substantially affected M2 formation.

Discussion

The major novel finding of this study is that tramadol is metabolized in dog liver to M1 by CYP2D15, whereas M2 is formed by multiple enzymes (primarily CYP2B11 and CYP3A12). Multiple observations

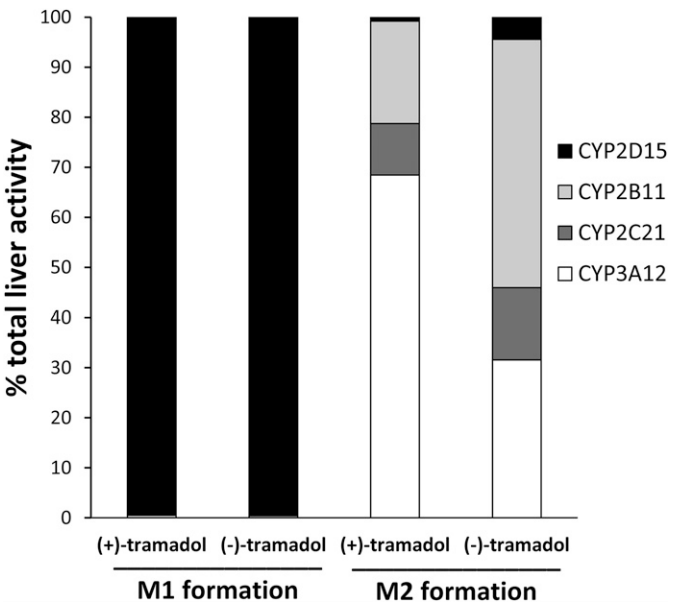

Fig. 7. Estimated relative contributions of canine P450s to M1 and M2 formation from tramadol in the liver from (+)-tramadol and from (−)-tramadol. Intrinsic clearance estimates from Table 2 were normalized to hepatic P450 content using average published estimates for CYP2B11, CYP2C21, CYP2D15, and CYP3A12 in Beagle liver microsomes. Note that this evaluation does not include a possible contribution from CYP2C41 since a hepatic abundance estimate was not available for this P450.

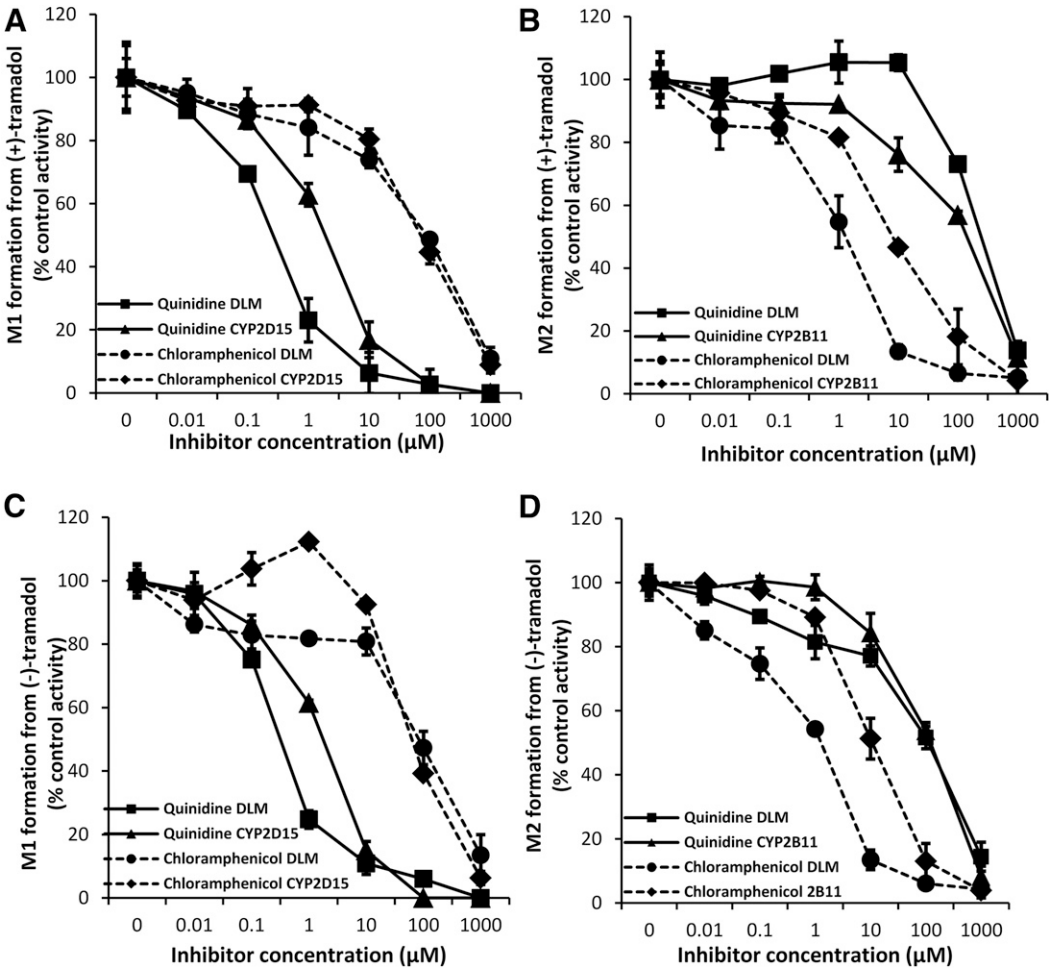

Fig. 8. Selective inhibition of M1 formation from (+)-tramadol (A) and (−)-tramadol (C) by quinidine in pooled (n = 27) DLMs and CYP2D15, and selective inhibition of M2 formation from (+)-tramadol (B) and (−)-tramadol (D) by chloramphenicol in pooled (n = 27) DLMs and CYP2B11. Shown are the rates of metabolite formation (mean ± S.D. of triplicate determinations) in the presence of inhibitor (0.01–1000 μM) expressed as a percentage of the formation rate without inhibitor (control activity).

provide evidence supporting these conclusions, including recombinant enzyme activities, selective inhibition of M1 formation by quinidine and of M2 formation by chloramphenicol and CYP2B11 antiserum, and induction of M2 formation (but not M1 formation) by phenobarbital. Recombinant enzyme activities also indicated minor contributions to M2 formation from CYP2C21 and CYP2D15 that account for <14% of liver activity when adjusted for published canine hepatic abundance of these P450s (Heikkinen et al., 2015). Recombinant CYP2C41 also showed significant M2 formation activity, especially from (+)-tramadol. Unfortunately, the hepatic protein abundance of CYP2C41 has not yet been reported, so the relative contribution of this enzyme to M2 formation in dog liver cannot be estimated currently. Although relatively little is known about CYP2C41, one study showed that only 4 of 25 dogs tested had the CYP2C41 gene, possibly resulting from a gene deletion polymorphism (Blaisdell et al., 1998). Consequently, one approach to evaluate the potential role of CYP2C41 in tramadol metabolism in dogs could involve comparing M2 formation in dogs with the CYP2C41 gene to those without.

Given the major role for CYP2D15 in M1 formation in dogs, it is likely that factors influencing CYP2D15 activity (e.g., genetic polymorphisms or coadministered CYP2D15 inducers or inhibitors) would influence circulating M1 concentrations. Various CYP2D15 genetic polymorphisms have been reported (Roussel et al., 1998; Paulson et al., 1999), although it is unclear whether they substantially affect CYP2D15 activity. We showed that quinidine is a relatively potent inhibitor of M1 formation by DLMs and CYP2D15; therefore, we would predict that coadministration of quinidine with tramadol would decrease its analgesic efficacy. However, this drug is not commonly used in dogs. Other potential CYP2D inhibitors that are more likely to be coadministered with tramadol for treatment of pain in dogs (e.g., buprenorphine, methadone, paroxetine, and fluoxetine) should be evaluated for effects on M1 formation.

Another important finding was the marked species difference in formation of M1 and M2 by dog, human, and cat liver microsomes. Based on published data on tramadol and metabolite plasma concentrations in dogs, we had hypothesized that M1 formation should be lowest with DLMs. Although we did confirm lower M1 formation compared with cats, M1 formation by DLMs was higher than for human liver microsomes. Consequently, additional mechanisms are likely to account for low M1 concentrations in dog plasma. One possibility is competition for substrate availability for *O*-demethylation to M1 by more rapid *N*-demethylation to M2. In support of this, we did show a much higher capacity for DLMs to form M2 compared with human and cat liver microsomes, suggesting that CYP2B11- and/or CYP3A12-mediated tramadol *N*-demethylation is much more efficient in dogs. Another possibility is more rapid clearance of M1 in dogs compared with cats and humans. M1 appears to be cleared largely via *N*-demethylation to M5, which is also a major circulating tramadol metabolite in dogs. Although

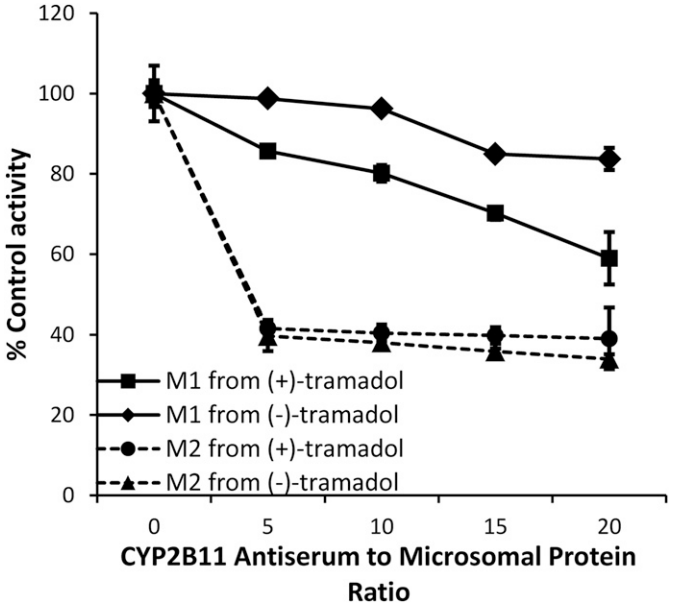

Fig. 9. Selective inhibition of M2 (but not M1) formation from (+)-tramadol and (−)-tramadol by anti-CYP2B11 immune serum in pooled (n = 27) DLMs. Shown are the rates of metabolite formation (mean ± S.D. of triplicate determinations) in the presence of anti-CYP2B11 immune serum (5:1 to 20:1 antiserum to microsome protein ratio) expressed as a percentage of the formation rate without antiserum (control activity).

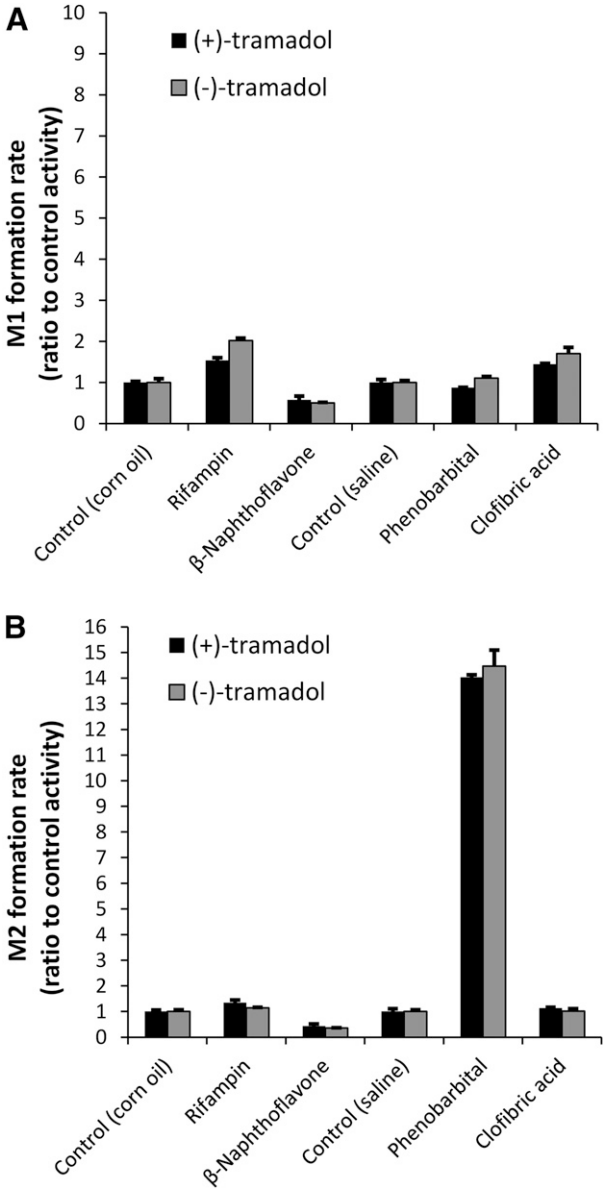

Fig. 10. Effect of P450 inducers on the rate of M1 (A) and M2 (B) formation from (+)-tramadol and (−)-tramadol in pooled liver microsomes from dogs treated with rifampin, β-naphthoflavone, phenobarbital, and clofibric acid. Shown are the rates of metabolite formation (mean ± S.D. of triplicate determinations) in microsomes prepared from inducer-treated male Beagle dogs (pooled from two dogs per treatment) expressed as a ratio of the formation rate in microsomes from vehicle-treated dogs (control activity).

M5 has weak μ-opioid receptor effects when administered directly into the brain, peripheral administration has no opioid effects, suggesting that it is unable to effectively cross the blood–brain barrier (Gillen et al., 2000). Consequently, this pathway (M1 conversion to M5) could be an important determinant of M1-dependent opioid effects; future studies are needed to evaluate this pathway, including identification of the responsible P450s.

Metabolism by P450s in the intestinal mucosa could also influence circulating concentrations of M1 and M2 through first-pass metabolism after oral administration of tramadol. A quantitative proteomics study recently showed that of seven P450s evaluated, CYP3A12 and CYP2B11 are the predominant P450s in canine intestinal mucosa (Heikkinen et al., 2015). However, CYP2D15 was not detected. Consequently, on the basis of our results, M2 formation is predicted to predominate over M1 formation in dog intestinal mucosa, which could be evaluated in future studies of dog intestinal microsome preparations.

Another interesting finding is that we observed non-Michaelis–Menten biphasic enzyme kinetics in Eadie-Hofstee plots of M1 and M2 formation by both DLMs and recombinant enzymes. Biphasic kinetics were reported previously in several other studies for tramadol metabolism by human liver microsomes (Paar et al., 1992; Subrahmanyam et al., 2001). This was attributed in one study to the contribution of multiple low- and high-affinity P450 isoforms to the measured activity (Subrahmanyam et al., 2001). However, we also observed biphasic kinetics for individual recombinant P450s; this instead suggests the presence of low- and high- affinity catalytic sites for tramadol within the same enzyme, although other causes cannot be excluded (Seibert and Tracy, 2014).

There was some evidence for stereoselectivity in tramadol metabolism, in that M1 was formed about two times more efficiently from (+)-tramadol than from (−)-tramadol by both DLMs and CYP2D15. This could be a reflection of differences in binding of (+)-tramadol versus (−)-tramadol to the CYP2D15 enzyme active site (or sites), thereby influencing catalytic efficiency. Both CYP3A12 and CYP2C41 also appeared to be more efficient at forming M2 from (+)-tramadol compared with (−)-tramadol, but this difference was not observed in DLMs. In contrast with our results, M1 formation from (+)-tramadol was previously shown to be about two times less efficient than M1 formation from (−)-tramadol in human (Paar et al., 1992) and rat (Liu et al., 2003) liver microsomes. Furthermore, higher M2 formation from (−)-tramadol compared with (+)-tramadol has been reported for human liver microsomes (Paar et al., 1992). These species differences probably reflect differences in binding of (+)-tramadol and (−)-tramadol to the respective P450 active sites between species. The clinical implications of these differences in the stereoselective metabolism of tramadol with regard to the analgesic effects of this drug remain to be determined.

In conclusion, the results of this study suggest that lower circulating concentrations of the tramadol M1 metabolite in dogs compared with humans and cats may be explained by more efficient formation of the tramadol M2 metabolite through a competing pathway. In addition, multiple approaches identified CYP2D15 as the predominant P450 mediating formation of M1, whereas M2 was formed mainly by CYP2B11 and CYP3A12 in canine liver.

Authorship Contributions

Participated in research design: Perez, Mealey, Grubb, Greene, Court.

Conducted experiments: Perez.

Performed data analysis: Perez, Court.

Wrote or contributed to the writing of the manuscript: Perez, Mealey, Grubb, Greene, Court.

References

Almeida RM, Escobar A, and Maguilnik S (2010) Comparison of analgesia provided by lidocaine, lidocaine-morphine or lidocaine-tramadol delivered epidurally in dogs following orchiectomy. *Vet Anaesth Analg* **37**:542–549.

Blaisdell J, Goldstein JA, and Bai SA (1998) Isolation of a new canine cytochrome P450 CDNA from the cytochrome P450 2C subfamily (CYP2C41) and evidence for polymorphic differences in its expression. *Drug Metab Dispos* **26**:278–283.

Cagnardi P, Villa R, Zonca A, Gallo M, Beccaglia M, Luvoni GC, Vettorato E, Carli S, Fonda D, and Ravasio G (2011) Pharmacokinetics, intraoperative effect and postoperative analgesia of tramadol in cats. *Res Vet Sci* **90**:503–509.

Cardozo LB, Cotes LC, Kahvegian MA, Rizzo MF, Otsuki DA, Ferrigno CR, and Fantoni DT (2014) Evaluation of the effects of methadone and tramadol on postoperative analgesia and serum interleukin-6 in dogs undergoing orthopaedic surgery. *BMC Vet Res* **10**:194.

Clark JS, Bentley E, and Smith LJ (2011) Evaluation of topical nalbuphine or oral tramadol as analgesics for corneal pain in dogs: a pilot study. *Vet Ophthalmol* **14**:358–364.

Court MH, Von Moltke LL, Shader RI, and Greenblatt DJ (1997) Biotransformation of chlorzoxazone by hepatic microsomes from humans and ten other mammalian species. *Biopharm Drug Dispos* **18**:213–226.

Davila D, Keeshen TP, Evans RB, and Conzemius MG (2013) Comparison of the analgesic efficacy of perioperative firocoxib and tramadol administration in dogs undergoing tibial plateau leveling osteotomy. *J Am Vet Med Assoc* **243**:225–231.

Delgado C, Bentley E, Hetzel S, and Smith LJ (2014) Comparison of carprofen and tramadol for postoperative analgesia in dogs undergoing enucleation. *J Am Vet Med Assoc* **245**:1375–1381.

Duignan DB, Sipes IG, Leonard TB, and Halpert JR (1987) Purification and characterization of the dog hepatic cytochrome P-450 isozyme responsible for the metabolism of 2,2′,4,4′,5,5′-hexachlorobiphenyl. *Arch Biochem Biophys* **255**:290–303.

Evangelista MC, Silva RA, Cardozo LB, Kahvegian MA, Rossetto TC, Matera JM, and Fantoni DT (2014) Comparison of preoperative tramadol and pethidine on postoperative pain in cats undergoing ovariohysterectomy. *BMC Vet Res* **10**:252.

Fliegert F, Kurth B, and Göhler K (2005) The effects of tramadol on static and dynamic pupillometry in healthy subjects–the relationship between pharmacodynamics, pharmacokinetics and CYP2D6 metaboliser status. *Eur J Clin Pharmacol* **61**:257–266.

García Quetglas E, Azanza JR, Cardenas E, Sádaba B, and Campanero MA (2007) Stereoselective pharmacokinetic analysis of tramadol and its main phase I metabolites in healthy subjects after intravenous and oral administration of racemic tramadol. *Biopharm Drug Dispos* **28**:19–33.

García-Quetglas E, Azanza JR, Sádaba B, Muñoz MJ, Gil I, and Campanero MA (2007) Pharmacokinetics of tramadol enantiomers and their respective phase I metabolites in relation to CYP2D6 phenotype. *Pharmacol Res* **55**:122–130.

Gaynor JS (2008) Control of cancer pain in veterinary patients. *Vet Clin North Am Small Anim Pract* **38**:1429–1448, viii.

Gillen C, Haurand M, Kobelt DJ, and Wnendt S (2000) Affinity, potency and efficacy of tramadol and its metabolites at the cloned human mu-opioid receptor. *Naunyn Schmiedebergs Arch Pharmacol* **362**:116–121.

Giorgi M, Del Carlo S, Saccomanni G, Łebkowska-Wieruszewska B, and Kowalski CJ (2009) Pharmacokinetic and urine profile of tramadol and its major metabolites following oral immediate release capsules administration in dogs. *Vet Res Commun* **33**:875–885.

Grond S, Meuser T, Uragg H, Stahlberg HJ, and Lehmann KA (1999) Serum concentrations of tramadol enantiomers during patient-controlled analgesia. *Br J Clin Pharmacol* **48**:254–257.

Hay Kraus BL, Greenblatt DJ, Venkatakrishnan K, and Court MH (2000) Evidence for propofol hydroxylation by cytochrome P4502B11 in canine liver microsomes: breed and gender differences. *Xenobiotica* **30**:575–588.

Heikkinen AT, Friedlein A, Matondo M, Hatley OJ, Petsalo A, Juvonen R, Galetin A, Rostami-Hodjegan A, Aebersold R, Lamerz J, et al. (2015) Quantitative ADME proteomics - CYP and UGT enzymes in the Beagle dog liver and intestine. *Pharm Res* **32**:74–90.

Kögel B, Terlinden R, and Schneider J (2014) Characterisation of tramadol, morphine and tapentadol in an acute pain model in Beagle dogs. *Vet Anaesth Analg* **41**:297–304.

Kongara K, Chambers JP, Johnson CB, and Dukkipati VS (2013) Effects of tramadol or morphine in dogs undergoing castration on intra-operative electroencephalogram responses and post-operative pain. *N Z Vet J* **61**:349–353.

KuKanich B and Papich MG (2004) Pharmacokinetics of tramadol and the metabolite O-desmethyltramadol in dogs. *J Vet Pharmacol Ther* **27**:239–246.

KuKanich B and Papich MG (2011) Pharmacokinetics and antinociceptive effects of oral tramadol hydrochloride administration in Greyhounds. *Am J Vet Res* **72**:256–262.

Lai J, Ma SW, Porreca F, and Raffa RB (1996) Tramadol, M1 metabolite and enantiomer affinities for cloned human opioid receptors expressed in transfected HN9.10 neuroblastoma cells. *Eur J Pharmacol* **316**:369–372.

Lamont LA (2008) Multimodal pain management in veterinary medicine: the physiologic basis of pharmacologic therapies. *Vet Clin North Am Small Anim Pract* **38**:1173–1186, v.

Liu HC, Wang N, Yu Y, and Hou YN (2003) Stereoselectivity in trans-tramadol metabolism and trans-O-demethyltramadol formation in rat liver microsomes. *Acta Pharmacol Sin* **24**:85–90.

Malek S, Sample SJ, Schwartz Z, Nemke B, Jacobson PB, Cozzi EM, Schaefer SL, Bleedorn JA, Holzman G, and Muir P (2012) Effect of analgesic therapy on clinical outcome measures in a randomized controlled trial using client-owned dogs with hip osteoarthritis. *BMC Vet Res* **8**:185.

Martins TL, Kahvegian MA, Noel-Morgan J, Leon-Román MA, Otsuki DA, and Fantoni DT (2010) Comparison of the effects of tramadol, codeine, and ketoprofen alone or in combination on postoperative pain and on concentrations of blood glucose, serum cortisol, and serum interleukin-6 in dogs undergoing maxillectomy or mandibulectomy. *Am J Vet Res* **71**: 1019–1026.

Mastrocinque S and Fantoni DT (2003) A comparison of preoperative tramadol and morphine for the control of early postoperative pain in canine ovariohysterectomy. *Vet Anaesth Analg* **30**: 220–228.

Matouskova O, Slanar O, Chytil L, and Perlik F (2011) Pupillometry in healthy volunteers as a biomarker of tramadol efficacy. *J Clin Pharm Ther* **36**:513–517.

Morgaz J, Navarrete R, Muñoz-Rascón P, Domínguez JM, Fernández-Sarmiento JA, Gómez-Villamandos RJ, and Granados MM (2013) Postoperative analgesic effects of dexketoprofen, buprenorphine and tramadol in dogs undergoing ovariohysterectomy. *Res Vet Sci* **95**:278–282.

Neves CS, Balan JA, Pereira DR, Stevanin H, and Cassu RN (2012) A comparison of extradural tramadol and extradural morphine for postoperative analgesia in female dogs undergoing ovariohysterectomy. *Acta Cir Bras* **27**:312–317.

Paar WD, Frankus P, and Dengler HJ (1992) The metabolism of tramadol by human liver microsomes. *Clin Investig* **70**:708–710.

Paulson SK, Engel L, Reitz B, Bolten S, Burton EG, Maziasz TJ, Yan B, and Schoenhard GL (1999) Evidence for polymorphism in the canine metabolism of the cyclooxygenase 2 inhibitor, celecoxib. *Drug Metab Dispos* **27**:1133–1142.

Pypendop BH, Siao KT, and Ilkiw JE (2009) Effects of tramadol hydrochloride on the thermal threshold in cats. *Am J Vet Res* **70**:1465–1470.

Raffa RB, Friderichs E, Reimann W, Shank RP, Codd EE, Vaught JL, Jacoby HI, and Selve N (1993) Complementary and synergistic antinociceptive interaction between the enantiomers of tramadol. *J Pharmacol Exp Ther* **267**:331–340.

Rialland P, Authier S, Guillot M, Del Castillo JR, Veilleux-Lemieux D, Frank D, Gauvin D, and Troncy E (2012) Validation of orthopedic postoperative pain assessment methods for dogs: a prospective, blinded, randomized, placebo-controlled study. *PLoS One* **7**:e49480.

Roussel F, Duignan DB, Lawton MP, Obach RS, Strick CA, and Tweedie DJ (1998) Expression and characterization of canine cytochrome P450 2D15. *Arch Biochem Biophys* **357**:27–36.

Seibert E and Tracy TS (2014) Different enzyme kinetic models. *Methods Mol Biol* **1113**:23–35.

Slanar O, Nobilis M, Kvetina J, Mikoviny R, Zima T, Idle JR, and Perlík F (2007) Miotic action of tramadol is determined by CYP2D6 genotype. *Physiol Res* **56**:129–136.

Stamer UM, Lehnen K, Höthker F, Bayerer B, Wolf S, Hoeft A, and Stuber F (2003) Impact of CYP2D6 genotype on postoperative tramadol analgesia. *Pain* **105**:231–238.

Subrahmanyam V, Renwick AB, Walters DG, Young PJ, Price RJ, Tonelli AP, and Lake BG (2001) Identification of cytochrome P-450 isoforms responsible for cis-tramadol metabolism in human liver microsomes. *Drug Metab Dispos* **29**:1146–1155.

Teixeira RC, Monteiro ER, Campagnol D, Coelho K, Bressan TF, and Monteiro BS (2013) Effects of tramadol alone, in combination with meloxicam or dipyrone, on postoperative pain and the analgesic requirement in dogs undergoing unilateral mastectomy with or without ovariohysterectomy. *Vet Anaesth Analg* **40**:641–649.

Address correspondence to: Dr. Tania E. Perez, Program in Individualized Medicine, Pharmacogenomics Laboratory, Department of Veterinary Clinical Sciences, Washington State University College of Veterinary Medicine, 100 Grimes Way, Pullman, WA 99164. E-mail: tperez@vetmed.wsu.edu